Noname manuscript No.
(will be inserted by the editor)

Plasma Diagnostics of the Interstellar Medium with Radio Astronomy

Marijke Haverkorn · Steven R. Spangler

Received: March 12, 2013 / Accepted: ——

Abstract We discuss the degree to which radio propagation measurements diagnose conditions in the ionized gas of the interstellar medium (ISM). The "signal generators" of the radio waves of interest are extragalactic radio sources (quasars and radio galaxies), as well as Galactic sources, primarily pulsars. The polarized synchrotron radiation of the Galactic non-thermal radiation also serves to probe the ISM, including space between the emitting regions and the solar system. Radio propagation measurements provide unique information on turbulence in the ISM as well as the mean plasma properties such as density and magnetic field strength. Radio propagation observations can provide input to the major contemporary questions on the nature of ISM turbulence, such as its dissipation mechanisms and the processes responsible for generating the turbulence on large spatial scales. Measurements of the large scale Galactic magnetic field via Faraday rotation provide unique observational input to theories of the generation of the Galactic field.

Keywords interstellar matter-Milky Way, 98.38.-j · plasmas-astrophysical, 95.30.Qd · turbulence-space plasma, 94.05.Lk

1 Introduction

The purpose of this article is to discuss how radio propagation measurements provide diagnostics of the interstellar medium (ISM). By radio propagation measurements, we mean those in which a radio astronomical observable (such as the interferometric visibility, or the polarization position angle) has been modified by

M. Haverkorn
Department of Astrophysics/IMAPP, Radboud University Nijmegen, P.O. Box 9010, 6500 GL Nijmegen, The Netherlands
Leiden Observatory, Leiden University, P.O. Box 9513, 2300 RA Leiden, The Netherlands
Tel.: +31-24-365 2809
E-mail: m.haverkorn@astro.ru.nl

S. Spangler
Department of Physics and Astronomy, University of Iowa
Tel.: +1-319-335-1948
E-mail: steven-spangler@uiowa.edu

a medium between the source of the radio waves and the radio telescope. In this paper, we will be interested in plasma media. These measurements provide rather direct information on the ionized gas density (strictly speaking, the electron density), the interstellar magnetic field, and (sometimes) indirect information on flow velocities in the interstellar medium.

In addition to information on the mean plasma properties of the interstellar medium such as $\langle n_e \rangle$ and $\langle \mathbf{B} \rangle$, these propagation observations yield information on turbulent fluctuations in the interstellar plasma. In fact, it can be argued that the information on interstellar plasma turbulence is the most unique contribution of this type of observation to studies of the ISM.

This paper is intended, in part, to serve a tutorial and review function. However, there have been numerous reviews in the past on the probing of the interstellar medium by radio propagation measurements, and the implications of those measurements for the astrophysics of the ISM (see, in particular, Uscinski 1977; Rickett 1977, 1990). There is no point in repeating the material already published in those papers. In the present article, we will make detailed reference to those papers to make a number of important points. At the same time, we will stress remaining, open questions about the interstellar plasma and its turbulence. In some cases, those questions have been actively discussed for many years. We will also clearly point out and discuss those topics in which radio propagation measurements provide crucial data for some of the issues of greatest importance in contemporary astrophysics.

An underlying theme of this paper will be the conceptual unity of plasma processes that occur in the interstellar medium, the solar corona, the interplanetary medium, and finally, experiments in plasma physics laboratories. In the last decade or two, plasma physics laboratory experiments have succeeded in illuminating processes which also occur in astrophysical plasmas. These experiments deal with processes which are at the basis of plasma astrophysics. A partial list of the experiments which are contributing a new dimension to plasma astrophysics are measurement of Faraday rotation in laboratory plasmas, and its use in diagnosing the basic properties and processes in those plasmas (Brower et al 2002; Ding et al 2003), observation of the nonlinear interaction of Alfvén waves (Carter et al 2006), and a number of experimental efforts to investigate the nature of magnetic field reconnection, a core process in astrophysics (e.g. Brown et al 2002; Zweibel and Yamada 2009; Yamada et al 2010). The unity of plasma physics and plasma astrophysics is exemplified by the interesting fact that the same radio propagation techniques, with the same radio telescopes, are, or can be, used to study the plasma physics of the interstellar medium, the corona, and the solar wind.

1.1 The Fundamentals: (1) Phases of the ISM

As has been noted for decades, the interstellar medium exists in a number of "phases" of different temperature, density, and ionization state. These different properties mean that fundamental plasma parameters such as the ion gyroradius, ion cyclotron frequency, plasma β, and Debye length differ from one phase to another. The different phases and their plasma parameters were discussed in, and summarized Table 1 of Spangler (2001). For ease of reference, this information is reproduced here as Table 1. An interesting recent contribution to the discussion

Table 1 Main Phases of the Interstellar Medium

Astronomical Name	Density (cm^{-3})	Temperature (K)
Molecular Cloud	$\geq 10^4$	≤ 70
Cold Neutral Medium (CNM)	10 - 100	~ 100
HII regions	5 - 10	8000
Warm Neutral and Ionized Mediua (WNM & WIM)	0.1 - 0.5	8000
Coronal (HIM)	10^{-3}	10^6

of phases of the ISM has been the advocacy of Heiles for a "fifth phase", which is partially ionized (Heiles 2011). We concur with Heiles that even a relatively small degree of ionization can profoundly alter the dynamics of a largely neutral gas. Many laboratory plasmas have a lower degree of ionization than some of the neutral phases of the ISM listed in Table 1. However, it seems that this "fifth phase" is largely the same as the WNM. The new development in Heiles (2011) is the recognition of the role played by the partial ionization. As pointed out there, all of the phases are probably plasmas, since even the cold, predominantly neutral phases have sufficient ionization to satisfy the traditional criteria of plasmas (Spangler 2001).

As has long been noted, the pressures of the less dense phases of the ISM are, very roughly, comparable at a value of 1.0×10^{-13}–1.0×10^{-12} dynes/cm^2 (Ferrière 1998; Tielens 2005). By this standard, molecular clouds and HII regions are overpressured. In the case of molecular clouds, the gravitational potential contributes to confinement of the gas. HII regions are overpressured, expanding entities. The other phases, Cold Neutral Medium (CNM), Warm Neutral Medium (WNM), Warm Ionized Medium (WIM), and Coronal Phase or Hot Ionized Medium (HIM) have roughly comparable pressures and may, in fact, be in pressure equilibrium. In addition, the magnetic pressure of the interstellar medium is comparable to the aforementioned gas pressures, with a value of $\simeq 1.4 \times 10^{-12}$ dynes/cm^2 for $B_{ISM} = 6 \times 10^{-6}$ G. Finally, the pressure corresponding to the energy density of the Galactic cosmic rays is also similar, $\simeq 1.0\times10^{-12}$ dynes/cm^2, suggesting equilibration between the forms in which the ISM can store energy. This whole situation is summarized in the textbook by Tielens (2005), where a value of $\simeq 0.5 \times 10^{-12}$ dynes/cm^2 is quoted for the gas phases of the ISM (CNM, WNM, WIM, and HIM), and a pressure of $\simeq 1.0 \times 10^{-12}$ dynes/cm^2 is assigned to both the magnetic and cosmic ray pressure.

The pressures and other properties of the various phases of the ISM, as well as the pressures of the interstellar magnetic field and cosmic rays were considered in detail by Ferrière (1998). Ferrière (1998) also estimated how these pressures would change with Galactocentric radius and altitude above the Galactic plane. For the Galactic location of the Sun, and in the Galactic plane, Ferrière (1998) estimates (see Figure 3 of that paper) a pressure of 6.0×10^{-13} dynes/cm^2 for the gas phase, and $\simeq 1.0 \times 10^{-12}$ dynes/cm^2 for both the magnetic and cosmic ray pressures.

The above considerations are relevant to the scope of this paper. Our view of the interstellar medium considers it as a dynamic plasma. Magnetohydrodynamics (MHD) describes the dynamics as an interaction of the gas and the magnetic field via pressure terms as discussed above and magnetic tension forces. In addition,

plasmas interact with energetic particles such as the cosmic rays through resonant interactions with plasma turbulence.

Among the important, recent developments in this field has been continued progress in specifying the strength of the interstellar magnetic field $\mathbf{B}_{ISM}$, and its dependence on gas density (Crutcher et al 2010). A plot of magnetic field strength (largely deduced through Zeeman effect measurements) versus gas density shows considerable scatter, and a trend towards larger values only for densities greater than about 300 cm^{-3}. Crutcher et al (2010) also infer a median magnitude of the interstellar magnetic field of 6 ± 1 μG. This is in agreement with equipartition estimates of the total magnetic field strength from synchrotron emission, and a factor of about three higher than the regular magnetic field component. At the present, there is no observational evidence for a change in the magnitude of $\mathbf{B}_{ISM}$ between different parts of the low density ISM.

1.2 The Fundamentals: (2) Radio Wave Propagation through the ISM

This paper will concentrate on two radio propagation effects, acting on small ($10^2 - 10^3$ km) scales and large (pc) scales, respectively. These are angular broadening of a compact or pointlike source due to density turbulence in the interstellar medium, and Faraday rotation of linearly polarized radio waves from a radio source embedded in the ISM, or from outside the Galaxy. We also briefly allude to other radio scintillation phenomena caused by small scale turbulence. In the latter topic, we include the signature of ISM turbulence in gradients of the polarization vector of synchrotron radiation.

1.2.1 Angular broadening of compact sources

The basic physics content of radio wave propagation through the ISM is to be found in the expression for the refractive index of radio waves in a plasma. This is discussed in the proceedings of previous meetings of the International Space Science Institute, i.e. Spangler (2001) and Spangler (2009). As discussed there, the refractive index depends on the plasma density and magnetic field. For radio wave propagation in the ISM, the magnetic field dependence is determined by the component of the magnetic field in the direction of wave propagation. The modification of the radio refractive index by the magnetic field is much smaller than the modification due to the plasma density. This is responsible for the well-known feature that radio propagation measurements primarily diagnose the plasma density of the ISM, with only a higher order contribution due to the Galactic magnetic field.

Turbulent fluctuations in the plasma density and magnetic field cause stochastic spatial and temporal fluctuations in the refractive index in the ISM. As a result, propagation through such a medium induces all manner of fluctuations in the received radio wave field (Uscinski 1977). The theory of how fluctuations in the refractive index generate corresponding fluctuations in properties of the wave electric field (various n-point correlations of the electric field) is generally attributed to Tatarski (1961). An excellent illustration of the effects of wave propagation through a random medium is given by dynamic spectra of pulsars, an example of

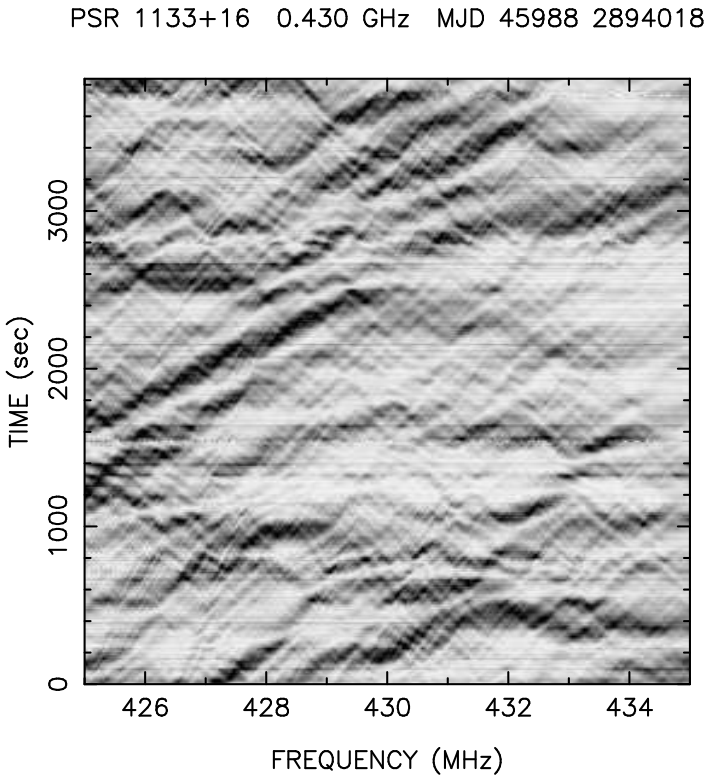

Fig. 1 A dynamic spectrum of the pulsar PSR1133+16. Wave propagation through the stochastic interstellar medium produces constructive and destructive interference at different spatial locations (here portrayed as time) and frequencies. Observations and figure provided by James Cordes, Cornell University.

which is shown in Figure 1[1] The spectrum of a pulsar is a measured as a function of time, and the set of spectra combined as shown in Figure 1. In the absence of the turbulent interstellar medium, the flux density of the pulsar would be constant over the frequency range shown. The gray scale indicates the brightness of the pulsar, with dark shaded regions being bright. The variation in brightness is due to scattered radio waves alternatively constructively and destructively interfering at different frequencies and times. A discussion of pulsar dynamic spectra and the information they contain is given in Cordes (1986). The specific observations shown in Figure 1 are discussed in Lazio et al (2004).

A major goal of the theory of wave propagation in a random medium is to relate, via an integral transform, the radio astronomical measurement as a function of the independent variable, to the density power spectral density as a function of wavenumber. Examples of major contributions to this literature are Uscinski (1977), Lee and Jokipii (1975), and Rickett (1977, 1990) . An illustration of the various types of observable stochastic propagation phenomena is given in Figure 1 of Spangler (2009).

[1] We thank James Cordes of Cornell University for providing this graph.

1.2.2 Depolarization and Faraday Rotation of Synchrotron radiation

Interstellar radio propagation measurements also provide information on the basic plasma state of the ISM, such as the plasma density, the vector magnetic field, as well as how these fields vary with position in the Galaxy.

Since variations in the magnetic field vector along the line of sight and/or within the angular size of a telescope beam will partially depolarize linearly polarized synchrotron emission, the observed degree of polarization traces the ratio of large-scale (regular) magnetic field strength to total magnetic field strength (Beck 2001). However, due to small-scale variations in this ratio due to local structure (supernova remnants, variable turbulence parameters), this method is mostly utilized on kpc-scales in external galaxies.

Parsec-size scales in the magnetized ISM are typically probed using Faraday rotation. The Faraday rotation measure RM is directly proportional to the path integral along the line of sight (los) of the electron density n_e and line-of-sight component of the magnetic field $B_\parallel$:

$$\left(\frac{RM}{\mathrm{rad\ m^{-2}}}\right) = 0.81 \int_{los} \left(\frac{n_e}{\mathrm{cm^{-3}}}\right) \left(\frac{B_\parallel}{\mu\mathrm{G}}\right) \left(\frac{dl}{\mathrm{pc}}\right) \quad (1)$$

Measurements of RM therefore provide nearly unique information on the magnetic field in the tenuous, ionized component of the ISM.

Traditionally, Faraday rotation is measured from the rotation of linear polarization angle θ as a function of wavelength $\theta = \theta_0 + RM\lambda^2$, where θ_0 is the intrinsic polarization angle at emission of the synchrotron radiation. An illustration of these ideas is given in Figure 2, which shows the Faraday rotation measure RM along several lines of sight to extragalactic radio sources in the Galactic plane in Cygnus. The Faraday rotation of the synchrotron radiation emitted by these sources is dominated by the Milky Way. The large differences in magnitude, and even sign, of RM between closely-spaced lines of sight in Figure 2 are an indicator of the role of young, luminous stars in this region, as they produce structure in the ISM via stellar winds and supernovae, and ionize the gas.

However, if synchrotron emission and the Faraday-rotating medium are mixed or alternating along the line of sight, the simple linearity of polarization angle change with λ^2 is no longer valid. This may be the case in the majority of Faraday rotation measurements. Faraday rotation measurements of the diffuse synchrotron emission in galaxies is the most obvious example, but extragalactic sources may also have several intrinsic RM components. In this case, every RM component i along the line of sight - now called Faraday depth ϕ_i to indicate that it only probes Faraday rotation along a part of the line of sight - adds its own polarization angle rotation of $\phi_i\lambda^2$, resulting in a non-linear polarization angle change with λ^2. However, this opens the possibility of a Fourier transform, with λ^2 as one of the conjugate variables, in order to disentangle the various ϕ_i components in the total observed signal. This method is called Rotation Measure synthesis (Burn 1966; Brentjens & de Bruyn 2005).

This Fourier transform relation between observed polarization vector as a function of wavelength squared $P(\lambda^2)$ and the Faraday dispersion function (or Faraday spectrum) is expressed as

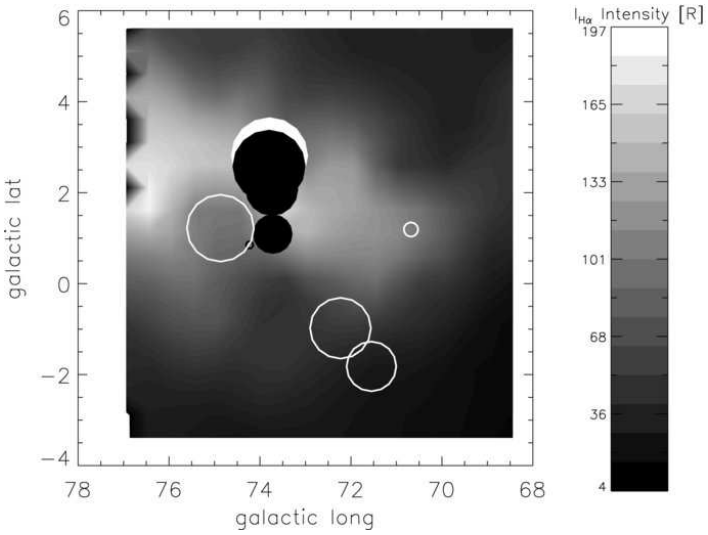

Fig. 2 Highly variable Faraday Rotation Measures in the Galactic plane in Cygnus, in the vicinity of the Cygnus OB1 star formation region. The sizes of the plotted circles are proportional to the magnitude of RM, specifically proportional to the logarithm of the absolute magnitude of RM. Filled circles correspond to positive RM, open circles are negative RM. The largest value of (absolute magnitude) of RM is 732 rad/m^2, and the smallest is 7.5 rad/m^2. The gray scale represents the intensity of $H\alpha$ emission in this region; the $H\alpha$ data may show the upper half of the plasma shell associated with the Cygnus OB1 association. Further discussion of these data is given in Whiting et al (2009). Figure taken from Whiting et al (2009), reproduced by permission of the American Astronomical Society.

$$P(\lambda^2) = \int_{-\infty}^{+\infty} F(\phi) \mathrm{e}^{2i\phi\lambda^2} d\phi \tag{2}$$

$$F(\phi) = \int_{\infty}^{+\infty} P(\lambda^2) \mathrm{e}^{-2i\phi\lambda^2} d\lambda^2 \tag{3}$$

However, since integration over wavelengths from $-\infty$ to $+\infty$ is not possible by definition, in practice these equations include a window function $W(\lambda^2)$ which is non-zero where there is wavelength coverage and zero elsewhere:

$$P_{obs}(\lambda^2) = W(\lambda^2)P(\lambda^2) = W(\lambda^2) \int_{-\infty}^{+\infty} F(\phi) \mathrm{e}^{2i\phi\lambda^2} d\phi \tag{4}$$

$$F_{obs}(\phi) = F(\phi) * R(\phi) = K \int_{\infty}^{+\infty} P_{obs}(\lambda^2) \mathrm{e}^{-2i\phi\lambda^2} d\lambda^2 \text{ where} \tag{5}$$

$$K = \left(\int_{\infty}^{+\infty} W(\lambda^2) d\lambda^2 \right)^{-1} \tag{6}$$

This introduces the Rotation Measure Spread Function (RMSF) $R(\phi)$, which describes sidelobes in the Faraday depth signal due to imperfect wavelength coverage, very analogous to the dirty beam (or point spread function) in radio interferometry due to imperfect coverage of the (u, v) plane.

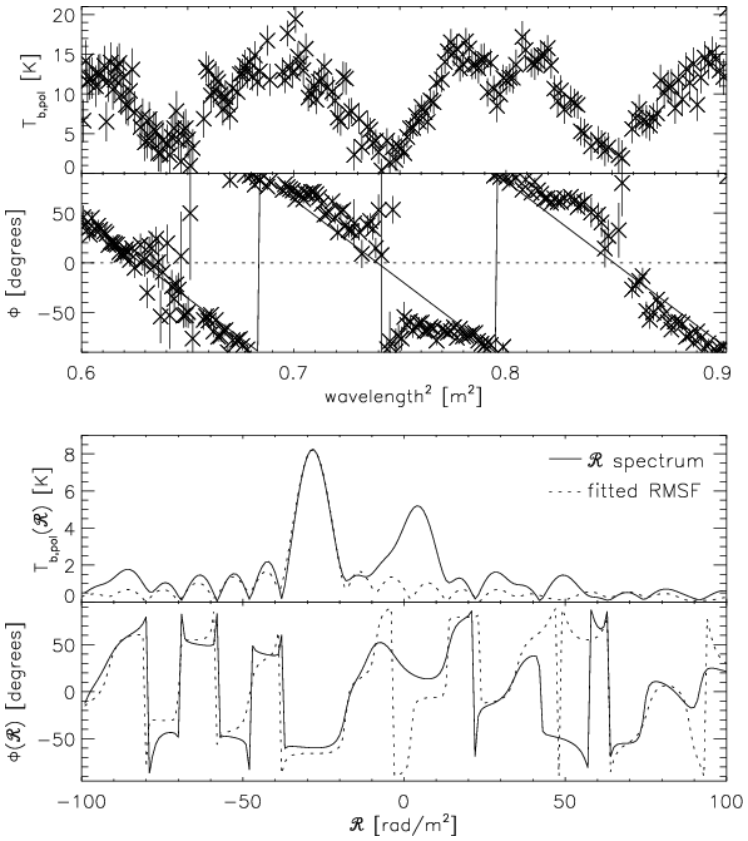

Fig. 3 Polarized intensity (top) and polarization angle (2nd from top) as a function of wavelength squared for synchrotron emission from an unnamed extragalactic point source. The Faraday spectrum (3rd from top) as a function of Faraday depth ϕ shows two peaks, indicating two separate Faraday depth components along this line of sight. Credit: Schnitzeler et al, A & A 494, 611, 2009, reproduced with permission ©ESO.

A nice illustration of this effect is given in Figure 3, which is taken from Schnitzeler et al (2009). The Figure shows polarized synchrotron intensity and polarization angle as a function of wavelength squared of an extragalactic point source. Variations in polarized intensity and non-linearity of polarization angle with λ^2 suggest that synchrotron emission and Faraday rotation are partially mixed. Indeed, the Faraday spectrum in the Figure shows two Faraday depth peaks belonging to two different synchrotron emitting regions with different amounts of Faraday rotation along the line of sight. The two Faraday depth components might both be due to the Galactic interstellar medium, or one might belong to a magneto-ionized medium in or around the extragalactic point source. Without additional information it is not possible to distinguish between these two possibilities.

2 Different Astrophysical Media, Common Phenomena

We point out the remarkable fact that a number of "astrophysical plasmas", i.e. distinct and very different media, have roughly similar radio propagation effects.

- The Faraday rotation measure (RM) due to the Earth's ionosphere is typically in the range $0.5 - 3$ rad/m^2. This is of the order of the RM due to the solar corona for lines of sight that pass at a heliocentric distance $\sim 10\ R_\odot$, and a factor of a few smaller than the standard deviation in RM of the interstellar medium at high Galactic latitudes Mao et al. (e.g. 2010).
- Very Long Baseline Interferometers operating at frequencies of 1 - 5 GHz measure similar effects, and of similar magnitude, when observing extragalactic radio sources through the inner solar wind at heliocentric distances of 10 - 30 $R_\odot$ or through the Galactic plane (Spangler and Sakurai 1995; Spangler et al 2002; Spangler and Cordes 1988; Fey et al 1991; Spangler and Cordes 1998).
- The fact that similar observational effects are measured for very different media means that scientists who study the ISM should be in dialog with heliospheric scientists who are studying related scientific questions.
- In the case of Faraday rotation, there is also a connection with laboratory plasma research. Faraday rotation is used as a diagnostic of fusion plasmas (Brower et al 2002; Ding et al 2003). This offers ISM astronomers the possibility of laboratory "ground truth" for some of our diagnostics.

3 Well-Established Results from Radio Propagation Studies

There are several results from radio propagation studies that are so well established, and confirmed by different investigators, that they now have the status of basic properties of the ISM that should be explained by theories.

3.1 "The Big Power Law in the Sky"

One of the best-known results from radio propagation studies is that the spatial power spectrum of density fluctuations follows a Kolmogorov spectrum over at least 5, and perhaps 10 decades (Armstrong et al 1995). It should be emphasized that the result of Armstrong et al (1995) pertains to the Warm Ionized Medium (WIM) component of the ISM. Analogous results have been reported for diagnostics of the neutral gas (e.g. Chepurnov et al 2010). The neutral gas resides in the WNM phase, which is spatially distinct from the WIM. As noted above, (Section 1.1) the degree of ionization in the WNM, while low, is not zero, and it may be considered as a weakly-ionized plasma. Whether the fluctuations studied by Chepurnov et al (2010) are driven by plasma dynamics due to the minority ion species remains unknown.

It is intriguing that the solar wind density power spectrum is the same as that observed for the ISM (at least for the slow solar wind), although the inertial subrange is smaller, being perhaps 3 orders of magnitude (Bruno and Carbone 2005). In the case of the ISM, it is perhaps not sufficiently appreciated that there must be a corresponding power law spectrum of magnetic field fluctuations to

explain the highly diffusive transport properties of cosmic rays with a very wide range of energies. This point has been made and emphasized by Jokipii (1977, 1988).

3.2 Spatial Variation in the Intensity of Interstellar Turbulence

A measure of the intensity of turbulence is the parameter C_N^2, which is the normalization constant of the density power spectrum. That is, if the spatial power spectrum of density fluctuations is $P_n(q)$ where q is the spatial wavenumber,

$$P_n(q) = C_N^2 q^{-\alpha} \tag{7}$$

and α is the spectral index of the power spectrum. This form of the power spectrum is the simplest, in which the power spectral density depends only on the magnitude of $\mathbf{q}$, and is thus isotropic. It is known that magnetohydrodynamic (MHD) turbulence is in fact anisotropic, with the large scale magnetic field determining the preferred direction (See comments in Section 3.4 below). In this case, the power spectral density $P_n(\mathbf{q})$ depends separately on $q_\perp$ and $q_\parallel$, the components of $\mathbf{q}$ perpendicular and parallel, respectively, to the large scale field (this is discussed in Spangler 1999, with a guide to the relevant literature). For most of this paper, we adopt Equation 7 as a convenient approximation.

The parameter C_N^2 is directly related to the variance of the density fluctuations. It has been long realized that C_N^2 varies drastically from one part of the interstellar medium to another (Rickett 1977; Cordes, Weisberg, and Boriakoff 1985). In some cases, it is clear that lines of sight with large C_N^2 traverse HII regions, or other regions with higher than normal plasma density. However, there appear to other lines of sight where no such obvious region of enhanced density exists. It remains unclear whether some of this variation could be due to true turbulent intermittency (Spangler and Cordes 1998; Spangler 1999).

3.3 The Galactic-Scale Magnetic Field

Large-scale Faraday rotation surveys of the sky show substantial organization of the RM in different parts of the sky, in the sense that the magnitude and sign of RM are correlated over significant parts of the sky. This is interpreted as evidence of a Galactic-scale magnetic field. Most likely, the large-scale magnetic field in the Milky Way generally follows the spiral arms, as is ubiquitously seen in synchrotron observations of external galaxies (Beck 2001). However, there is some evidence for local deviations from the spiral structure (Brown et al. 2007; Rae & Brown 2010; Van Eck et al. 2011), similar to M51 (Patrikeev et al. 2006). One reversal in the large-scale magnetic field direction just inside the Solar circle has been known for decades (e.g. Thomson & Nelson 1980), although it remains unclear why these large-scale reversals are not observed in external spirals. There is still much controversy about the number and location of any other large-scale field reversals in the Galactic disk. For an extensive review, see Haverkorn (2013).

3.4 Anisotropy of Turbulence

A major result from the theory of magnetohydrodynamic (MHD) turbulence, confirmed by observations of turbulence in the solar corona and solar wind, is that turbulence is anisotropic, in the sense of turbulent irregularities being stretched out along the large scale magnetic field. This result was obtained by Strauss (1976) for the case of irregularities in fusion plasmas, but the arguments presented by Strauss are also valid in the case of astrophysical plasmas. This property is also present in interstellar turbulence (see Brisken et al 2010; Rickett 2011, for recent discussions of the more pronounced cases).

3.5 The Dissipation Range of Turbulence

Important progress has been made in the past decade in our understanding of the dissipation of plasma turbulence. This progress has been possible through improved measurements of solar wind turbulence, as well as novel theoretical developments (Howes et al 2008; Alexandrova et al 2009; Howes et al 2011,2011; Sahraoui et al 2012). These investigations have identified spatial scales on which dissipation occurs, and advanced suggestions for the mechanisms by which this occurs. It is now clear that a break in the power spectrum of magnetic field fluctuations in the solar wind occurs on scales comparable to, and smaller than the ion inertial length l_i,

$$l_i \equiv \frac{V_A}{\Omega_i} \tag{8}$$

where V_A is the Alfvén speed and Ω_i is the ion (proton) cyclotron frequency (Howes et al 2011; Alexandrova et al 2009). There remains active discussion in the community as to whether the dissipation is due to Landau damping of highly oblique Alfvén waves (the assumption being that turbulent fluctuations on these scales have damping properties similar to linear plasma wave modes (Howes et al 2008, 2011,2011)), dissipation of other, higher frequency modes propagating at large angles with respect to the mean magnetic fields (Sahraoui et al 2012), or damping by other modes on electron inertial scales (Alexandrova et al 2009). In keeping with the philosophy of this paper, we assume that these results are of great importance of our understanding of the ISM as well.

As will be discussed in Section 4, there is now good evidence for the beginning of the dissipation range in interstellar turbulence at the ion inertial length, although there is also evidence for differences between solar wind and interstellar turbulence (see Section 4.5 below).

3.6 The Outer Scale of Interstellar Turbulence

The outer scale to magnetized turbulence in the Warm Ionized Medium (WIM) phase of the ISM is measured from structure functions of RM to be a few parsecs in the spiral arms, but up to ~ 100 pc in the interarm regions (Haverkorn et al 2006, 2008). This is in agreement with estimates of the outer scale of turbulence averaged over large parts in the sky (mostly towards the Galactic halo) of order 100 pc by Lazaryan & Shutenkov (e.g. 1990); Ohno & Shibata (e.g. 1993);

Chepurnov and Lazarian (e.g. 2010). These scales are similar to the final sizes of supernova remnants, suggesting (combined with energy arguments, see MacLow (2004)) that these are the dominant sources of turbulence in the WIM. The smaller outer scale found in spiral arms may be due to the abundance of H II regions (Minter & Spangler 1996; Haverkorn et al 2004). Small outer scales of a few parsecs have also been found in the highly polarized Fan region (Iacobelli et al. 2013) or from anisotropies in TeV cosmic ray distributions (Malkov et al. 2010).

4 Turbulent Microscales in the Interstellar Medium

4.1 Definition of Turbulent Microscales

In this section, we discuss the ways we can measure turbulence on very small scales in the interstellar medium. By very small scales, we mean those in the dissipation range. Knowledge of this part of the turbulent cascade is very important because it contains information on the way in which energy is taken from the large scales, on order of parsecs or more, and transferred to other forms, presumably heat energy of the interstellar gas.

Our interest in this section will be particularly focused on two phases of the ISM, the WIM and HII regions surrounding young stars. The WIM is of interest because it appears to be the best-diagnosed phase of the ISM, in the sense of a plasma physics measurement, primarily as a result of investigations done at the University of Wisconsin using Fabry Perot interferometers as very high spectral resolution spectrometers (see Haffner et al 2003, for a recent summary of this work.).

4.2 Turbulent Microscales in the Solar Wind

Once again, we use the solar wind, with its extensive and often sophisticated, in-situ measurements and substantial body of theoretical results as a model for interstellar turbulence. Spacecraft instruments provide in-situ measurements of virtually all plasma parameters of interest, and provide the best data set for discussions of MHD turbulence. Measurements of solar wind turbulence at a heliocentric distance of 1 a.u. (the bulk of spacecraft measurements) show a power-law power spectrum of magnetic field fluctuations with a single spectral index that extends from an outer scale with a size of one to a few solar radii, down to an inner scale of a few thousand kilometers (e.g. Bruno and Carbone 2005). A number of investigations have shown that this scale corresponds to the ion inertial length l_i defined in Equation 8.

Radio propagation observations through the corona and inner solar wind (Coles and Harmon 1989; Harmon and Coles 2005; Spangler and Sakurai 1995) also show strong evidence for an enhancement in the power spectral density of plasma density fluctuations on the scale of the ion inertial length. This bulge on the approximate scale of the ion inertial length can also be seen in power spectra from in-situ measurements of plasma density in the solar wind at 1 a.u. (Chen et al 2012). These observations, both from direct, in-situ measurements as well as radio propagation observations, are interpreted as evidence that the fluctuations in the dissipation

range have properties of obliquely-propagating, kinetic Alfvén waves, since such waves become more compressive at the ion inertial scale (Harmon 1989). In fact, the kinetic Alfvén nature of the fluctuations on the dissipation scale is the basis of the model of turbulence in the dissipation range advanced by Howes and colleagues (Howes et al 2011). So, the situation for the solar corona and solar wind seems quite consistent as regards both measurements of plasma density fluctuations and theoretical understanding of the entire turbulent cascade. The prominence of this directly-detected bulge appears to be less pronounced than that retrieved from radio propagation measurements in the corona and inner solar wind. This may indicate that the kinetic Alfvén wave component decays with increasing heliocentric distance in the solar wind. This would hardly be surprising, since many properties of the solar wind change with heliocentric distance (e.g. Bruno and Carbone 2005).

4.3 How We Measure Microscales in Interstellar Turbulence

The ion inertial length in the WIM phase of the interstellar medium is of order hundred to a few hundred kilometers (Spangler and Gwinn 1990). At first, it seems amazing that any kind of astronomical measurement, made on a medium with an extent of kiloparsecs, could diagnose fluctuations on such a scale. Radio propagation measurements make this possible.

The subsequent discussion in this section will concentrate on one of the scintillation phenomena mentioned in Section 1.2, angular broadening. A point source of radio waves viewed through a turbulent medium will appear as a blurred, fuzzy object. Essentially the same phenomenon is encountered at optical wavelengths in the form of seeing disks of stars. A radio source that is blurred by interstellar turbulence will have a measured brightness distribution $I(x, y)$ which is more extended than the intrinsic image of the source. This brightness distribution contains information on the intensity and spatial power spectrum of the density fluctuations. Here I is the intensity of the radiation, which is a function of two angular coordinates on the sky, x and y, customarily Right Ascension and Declination. The brightness distribution is related to the observable quantity which is directly measured by the interferometer. The way a radio interferometer makes an image of a radio source is to measure the *complex visibility function* $V(u, v)$, which is directly related to the correlation between the radio wave electric field at two antennas of an interferometer (Thompson et al 1986). The complex visibility function has units of Janskys (radiative flux), and is a function of the arguments u and v, the east-west and north-south components of the interferometer baseline, normalized by the wavelength of observation. A two dimensional Fourier transform relates the complex visibility function $V(u, v)$ and $I(x, y)$ (Thompson et al 1986).

Observations have shown that the turbulent irregularities in the WIM and HII regions around OB associations, like those in the corona and solar wind, are anisotropic in the sense that is theoretically expected. A summary of the observational evidence as of 1999 is given in Spangler (1999). For the present purposes, we will employ the approximation of isotropic irregularities. The arguments given here can be generalized to the case of anisotropic scattering (Spangler and Cordes

1988). In the case of isotropic scattering,

$$V(u,v) = V(\sqrt{u^2+v^2}) = V(r) \tag{9}$$

where r is the (dimensional) interferometer baseline length, projected on the plane of the sky. In this case, the complex visibility function of a point source viewed through a turbulent medium is a real function, (Cordes, Weisberg, and Boriakoff 1985; Spangler and Gwinn 1990)

$$V(r) = S_0 e^{-\frac{1}{2}D_\phi(r)} \tag{10}$$

where S_0 is the total flux density of the source, and $D_\phi(r)$ is the *phase structure function*, which contains information on the intensity and spatial power spectrum of the density fluctuations. For the case of scattering by a homogeneous, turbulent slab of thickness L, the phase structure function is (Cordes, Weisberg, and Boriakoff 1985; Spangler and Gwinn 1990)

$$D_\phi(r) = 8\pi^2 r_e^2 \lambda^2 L \int_0^\infty dq q \left[1 - J_0(qr)\right] P_n(q) \tag{11}$$

The functions and variables in Equation 11 are as follows. The classical electron radius is given by r_e, λ is the wavelength of observation, L is the thickness, or extent along the line of sight of the turbulent plasma, q is the magnitude of the turbulent wavenumber, $J_0(x)$ is a Bessel function of the first kind of order 0, and $P_n(q)$ is the spatial power spectrum of the density fluctuations. One expects the power spectra of all plasma parameters to be modified at wavenumbers corresponding to the reciprocal of the ion inertial length, ion gyroradius, or similar plasma microscale on which dissipation begins to become important. Spangler and Gwinn (1990) adopted the following simple model in which Equation 7 is modified by having the power spectrum truncated on wavenumbers larger than a dissipation wavenumber q_0,

$$P_n(q) = C_N^2 q^{-\alpha} e^{-q/q_0} \tag{12}$$

Although Equation 12 is highly simplified, and was adopted by Spangler and Gwinn (1990) for analytic convenience, the power spectrum of magnetic field fluctuations in the solar wind at 1 AU is truncated by an exponential function (Alexandrova et al 2009, see also presentation by Alexandrova et al in this meeting). An important difference between the result of Alexandrova et al (2009) and the analysis presented below is that Alexandrova et al (2009) found exponential truncation of the power spectrum on electron rather than ion scales (i.e. electron inertial length, or electron gyroradius).

Substitution of Equation 12 into Equation 11, and change of variables from $q \rightarrow y \equiv qr$ gives the following expression

$$D_\phi(r) = 8\pi^2 r_e^2 \lambda^2 (C_N^2 L) r^{\alpha-2} \int_0^\infty dy \left[1 - J_0(y)\right] y^{-(\alpha-1)} e^{-y/Q} \tag{13}$$

where $Q \equiv \frac{r}{l_d}$, where l_d is the dissipation scale, $l_d \simeq \frac{1}{q_0}$. The quantity $C_N^2 L$ is termed the *scattering measure*, and roughly determines the magnitude of angular broadening. Turbulent plasmas that have large C_N^2, large L, or both, will produce heavy angular broadening.

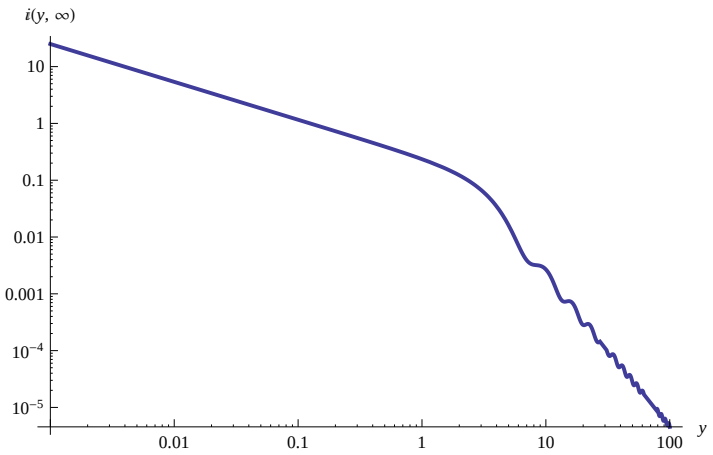

Fig. 4 Plot of the function $I(y, Q)$ for a Kolmogorov spectrum ($\alpha = 11/3$) and $Q = \infty$. The integrand tells what wavenumbers in the turbulent spectrum dominate the measurement on a given interferometer baseline. This occurs for $y \equiv qr \geq 1$, which corresponds to irregularities with sizes of order the interferometer baseline.

Equation 13 yields important insight on remote sensing diagnosis of interstellar (and heliospheric) turbulence. Let us start with the case $Q \to \infty$, which corresponds to an infinitely small dissipation scale. In this case, the spectrum is power law for all wavenumbers larger than that corresponding to the outer scale. In this case, the integral in Equation 13 is a number which depends only on the index α. For the Kolmogorov spectrum ($\alpha = 11/3$) the value of the integral is 1.117, and the structure function $D_\phi(r) \propto r^{5/3}$.

Equation 13 also illustrates one of the most intriguing aspects of radio wave propagation, and demonstrates why radio astronomical measurements can contribute much to a discussion of plasma microscales in the ISM. Since Equation 13 is an integral over wavenumber (this is explicit in Equation 11), the integrand shows which wavenumbers dominate the measurement. The integrand in Equation 13, which we note by the function $I(y, Q)$, is shown in Figure 4 for the case $I(y, \infty)$ and $\alpha = 11/3$ (Kolmogorov spectrum).

The function $I(y, \infty)$ is monotonically decreasing with increasing y. At first, this would seem to indicate that the lowest wavenumbers in the spectrum dominate the measurement. However, that is not true for the case of a Kolmogorov spectrum. The measurement (D_ϕ) is determined by an integral over y. This is because for $y \leq 2$, each progressively higher decade in y makes a larger contribution to the integral. The integral is dominated by contributions with $y \sim 1 - 10$ where there is an inflection in the function $I(y, \infty)$. When an interferometer measures a broadened radio source, it is responding to irregularities with a wide range of wavenumbers. However, the dominant contribution to the visibility measurement is from irregularities with sizes comparable to the baseline length. This baseline length ranges from tens of kilometers in the case of the Very Large Array, to a few thousand kilometers in the case of Very Long Baseline Interferometers. Obviously, for this statement to be relevant, a measurement with a given interferometer must be affected or even dominated by propagation effects. This point was made in the context of interstellar scattering in Spangler (1988).

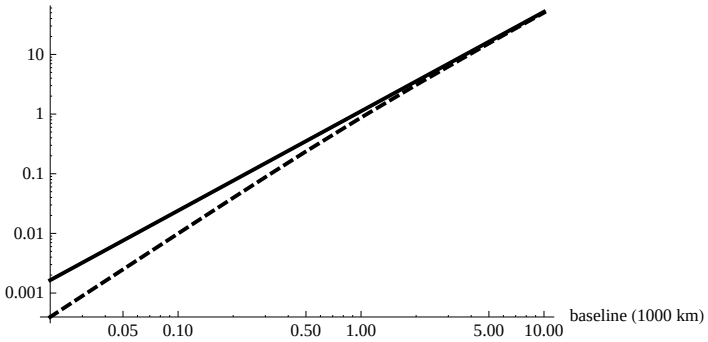

Fig. 5 Theoretical structure functions of turbulence in the interstellar medium. The plotted lines correspond to theoretical structure functions $D_\phi(r)$ given by Equation (10). Both adopt a Kolmogorov spectrum of density irregularities. The solid curve is for a Kolmogorov spectrum with no inner scale ($l_d \rightarrow 0$). The dashed line corresponds to a spectrum with an inner scale $l_d = 300$ km. Sensitive, carefully calibrated interferometer measurements can distinguish between these two cases.

Equation 13 also shows how the presence of turbulent dissipation is manifest in radio propagation measurements. When Q is finite, corresponding to a finite dissipation scale, the $e^{-y/Q}$ term will depress the value of the integral. The value of $D_\phi(r)$ at short baselines, where dissipation is pronounced, is less than a value extrapolated from larger values of r according to an $r^{5/3}$ relation. In the dissipation range, $D_\phi(r)$ has a steeper dependence than $r^{5/3}$. To illustrate these points, Figure 5 shows two structure functions, one without an inner scale and the other with an outer scale of 300 km.

4.4 Observational Results on Turbulent Dissipation Scales in the Interstellar Medium

These issues were discussed in Spangler and Gwinn (1990), who showed that observers who interpret their angular broadening data in terms of a spectral index α would report values which depend on the baselines used in the measurement. Angular broadening measurements on short baselines would yield a value of $\alpha \simeq 4.0$, whereas measurements on long baselines in the inertial subrange would yield $\alpha \simeq 3.67$. This may be seen by reference to Figure 5. The inferred spectral index is determined by the slope of $D_\phi(r)$ versus r on a log-log plot, such as Figure 5. Spangler and Gwinn (1990) assembled the data on angular broadening measurements that were available at that time, and showed that a dependence of the inferred value of α on the interferometer baselines used did seem to be present in the data. The result was shown in Figure 1 of Spangler and Gwinn (1990). From these data they found that there could be a break in the interstellar density power spectrum with an inner scale of 50 - 200 km. More importantly, they pointed out that a scale in this range was actually expected, if the inner scale corresponds to the ion inertial length l_i defined in Equation 8, as is the case for scattering in the corona and solar wind (Section 4.2).

A more direct determination of an inner scale, made from comparison of measured $D_\phi(r)$ values with the theoretical expression in Equations (10) and (12),

was made by Molnar et al (1995). Molnar et al (1995) made and analyzed angular broadening measurements similar to those of Spangler and Cordes (1988), but of the radio source Cygnus X-1. It is viewed through the HII region associated with the Cygnus OB2 association. Molnar et al (1995) essentially made a fit of Equation (10) (but including the effect of anisotropy of scattering) to their data, and found a satisfactory model to be a Kolmogorov underlying spectrum and an inner scale of 300 kilometers.

An additional, and particularly compelling result has been the recent report by Rickett et al (2009). They studied the form of the broadening profile of pulses of the pulsar PSRJ1644-4559 late in the pulse. At this time, radiation is being received from highly scattered rays that are probing very small scale irregularities. Rickett et al (2009) make the important point that the amount of radiation received late in the pulse is only consistent with a Kolmogorov spectrum that breaks at an inner scale as expressed by Equation 12, or something similar. A power spectrum that remained Kolmogorov to infinitely high spatial wavenumber would cause more pulse power to be observed late in the pulse than is actually seen. Rickett et al (2009) use their data to extract a value for the inner scale of 70 - 100 km.

These three independent investigations using radio propagation data have therefore concluded that there is a spectral break in the density power spectrum of the interstellar medium, and that this inner scale is consistent with the ion inertial length. It should be emphasized that the lines of sight analyzed by Spangler and Gwinn (1990), Molnar et al (1995), and Rickett et al (2009) all traversed HII regions. There is, as yet, no observational data that can determine the inner scale to the turbulence in the WIM. We do not know if such an inner scale would be at the ion inertial length.

4.5 A Break or a Bulge?

One interesting, and at the present preliminary feature emergent from these investigations regards the transition to the dissipation range in interstellar turbulence. In HII region plasmas, the dissipation range appears to consist of a smooth steepening, without the bulge in the density power spectrum on the ion inertial length, as exists in the corona and solar wind (Section 6.1). Given the admittedly limited present information, it appears that the interstellar spectrum of density fluctuations has no compressive bulge at the inner scale. If confirmed by subsequent investigations, it could point to an important distinction between turbulence in the interstellar medium and that in the solar corona and solar wind. The results from Rickett et al (2009) seem particularly compelling, because a bulge in the interstellar density power spectrum on the ion inertial scale would produce more pulse power at late arrival times than is actually seen (this point is clearly illustrated in Figure 7 of Rickett et al (2009)).

If this bulge is missing in the interstellar density spectrum, what does it signify? Does it imply that kinetic Alfvén waves are not present in the turbulent field, or that the small scale irregularities in the interstellar medium do not evolve in a manner similar to kinetic Alfvén waves? In that case, what is the nature of the fluctuations over such a large inertial subrange in the ISM? As mentioned in Section 4.2, the solar wind results may provide guidance; the results of Chen et al

(2012) indicate that the prominence of kinetic Alfvèn waves decreases with increasing heliocentric distance. Interstellar turbulence is comparatively much older in terms of the number of eddy turnover times, so it is certainly plausible that the kinetic Alfvèn wave component of ISM turbulence has dissipated.

These ruminations need more extensive and more convincing observational demonstration. Fortunately, the instruments and observational techniques are operational and available. The instruments currently available for angular broadening measurements are greatly improved over those used in the measurements cited above (Spangler and Cordes 1988; Spangler and Gwinn 1990; Molnar et al 1995; Spangler and Cordes 1998). Those investigations used Very Long Baseline Interferometers with much smaller bandwidths and correlator capability than are now available with the Very Long Baseline Array (VLBA) of the National Radio Astronomy Observatory (NRAO). In addition, the LOFAR low frequency radio telescope in Europe is now operational and has the capability of making novel angular broadening measurements. Finally, the work of Rickett et al (2009) also demonstrates the advances that have been made in pulsar measurements of the ISM, utilizing new, state-of-the-art pulsar processors on large single dish telescopes such as the Parkes antenna or the Green Bank Telescope of NRAO. Future investigations with these powerful new instruments could illuminate the interesting question as to whether turbulent dissipation processes are the same in the solar wind and the plasma components of the interstellar medium.

5 Turbulent mesoscales in the interstellar medium

5.1 Rotation Measure Synthesis results

The interpretation of three-dimensional Faraday depth cubes (i.e. intensity maps in spatial coordinates where Faraday depth is the third dimension) is anything but straightforward.

In addition to the artefacts introduced by a non-Gaussian rotation measure spread function, as explained in Section 1.2.2, a number of other effects contribute to the difficulty of translating rotation measure cubes into physical properties of the interstellar medium.

Firstly, in analogy to aperture synthesis, a limited range in wavelength squared causes a limited sensitivity to large-scale Faraday depth structures. In contrast with aperture synthesis, in RM synthesis this can lead to a situation where the maximum detectable scale is smaller than the Faraday depth resolution. Therefore, only Faraday-thin components[2] and sharp gradients in Faraday depth, such as the edges of Faraday-thick components, will show up in a Faraday spectrum. The dependence on wavelength range of the Faraday depth resolution $\delta\phi$, maximum detectable scale $\Delta\phi_{max}$ and maximum detectable Faraday depth ϕ_{max} are given by Brentjens & de Bruyn (2005) as

[2] Faraday-thin component is defined as a gaseous medium observed at a wavelength where the change of polarization angle through Faraday rotation is small. Brentjens & de Bruyn (2005) define Faraday-thin as $\phi\lambda^2 << 1$ and Faraday-thick as $\phi\lambda^2 >> 1$. A Faraday-thin component displays negligible internal Faraday depolarization.

$$\delta\phi \approx \frac{2\sqrt{3}}{\Delta\lambda^2} \tag{14}$$

$$\Delta\phi_{max} \approx \frac{\pi}{\lambda^2_{min}} \tag{15}$$

$$|\phi_{max}| \approx \frac{\sqrt{3}}{\delta\lambda^2} \tag{16}$$

Secondly, different Faraday depth features in a Faraday spectrum only contain information about the amount of their Faraday depth, but not necessarily about their distance. If along a line of sight Faraday depth increases monotonically, i.e. if no magnetic field reversals exist along the line of sight, then the distance order of Faraday depth components is known. However, in the general ISM, with many multi-scale magnetic field reversals, distance to Faraday components is usually unknown. Only in exceptional cases, if one has complementary rotation measures from a number of pulsars with known distances along similar lines of sight, or if the Faraday depth component has a counterpart with a known distance in another tracer, is it possible to estimate the distance to a Faraday component.

Taking these caveats into account, a number of studies on RM synthesis of diffuse Galactic synchrotron emission have been done, which show mostly consistent results. Brentjens (2011) examines a $\sim 4^\circ \times 7^\circ$ field around the Perseus galaxy cluster, which mostly displays Galactic synchrotron emission, at a broad frequency range around 350 MHz. Synchrotron emitting components are detected at multiple Faraday depths between -50 and $+100$ rad m^{-2}, are Faraday thin and spatially thin ($\leq$ 40 pc), and are well separated in Faraday depth space, suggesting that they are flanked by Faraday-rotating-only parts of the ISM.

The same effect is noticed by Iacobelli et al. (2013), who study the "ring stucture" in the Fan region (see e.g. Haverkorn et al 2003; Bernardi et al 2009) in RM synthesis around 150 MHz. They also identify separate Faraday depth components, viz. the ring structure and a foreground component which they associate with the Local Bubble. Similarly, Pizzo (2010) notice in their Galactic foreground studies in the direction of the galaxy cluster Abell 2255 at multiple frequency bands from 150 MHz to 1200 MHz three distinct ranges of Faraday depth with widely different morphologies.

These early RM synthesis studies of Galactic diffuse synchrotron emission consistently conclude that the synchrotron emission is visible in detected in discrete, often Faraday thin, structures with widely different morphologies, interspersed with Faraday-rotating-only components. It is tempting to interpret these observations as actual small-scale variability in synchrotron emission in the ISM, or discrete regions of excess emission. However, two other effects are at play as well. Synchrotron emission dominates in locations where $\mathbf{B} = \mathbf{B}_\perp$, while Faraday rotation only depends on $B_\parallel$. This may cause the observed apparent anti-correlation between synchrotron emission and Faraday rotation. Secondly, the insensitivity of the technique to large Faraday-thick (emitting and Faraday rotating) structures, which may mimic Faraday-thin emission components at the edges of the Faraday depth range, will play a role.

Wavelet analysis can be successfully applied to Faraday depth cubes to recognize magnetic features such as turbulence or large-scale magnetic field reversals in nearby spiral galaxies or the intracluster medium in galaxy clusters (Beck et al

2012). Low frequency data (~ 100 MHz) are needed to provide the necessary Faraday depth resolution, while broad frequency coverage (up to several GHz) is crucial to make broad Faraday structures detectable. In practice this requires combination of broad-band data from various telescopes, such as the Global Magneto-Ionic Medium Survey (GMIMS, Wolleben et al 2009).

5.2 Polarization gradients

Linearly polarized intensity maps of diffuse synchrotron emission consistently show narrow one-dimensional structures of complete depolarization named *depolarization canals* (Haverkorn et al. 2000). Some of these depolarization canals are observational artefacts due to missing short spacings in radio interferometric observations, while other canals point to locations of sharp jumps in rotation measure, i.e. sudden changes in electron density and/or parallel magnetic field in the ISM (Shukurov & Berkhuijsen 2003; Haverkorn et al. 2004). In addition, not all of these sudden changes in ISM conditions are visible as depolarization canals.

The method of gradients in linear polarization was devised to obtain a complete census of these locations of sudden change of conditions in the ISM (Gaensler et al. 2011). The vectorial polarization gradient is calculated from the Stokes parameters (Q, U) as

$$|\nabla \mathbf{P}| = \left\{ \left(\frac{\partial Q}{\partial x}\right)^2 + \left(\frac{\partial Q}{\partial y}\right)^2 + \left(\frac{\partial U}{\partial x}\right)^2 + \left(\frac{\partial U}{\partial y}\right)^2 \right\}^{1/2} \tag{17}$$

This gives a random-looking pattern of mostly one-dimensional locations of high polarization gradient, of which depolarization canals are a subset (see Fig. 6).

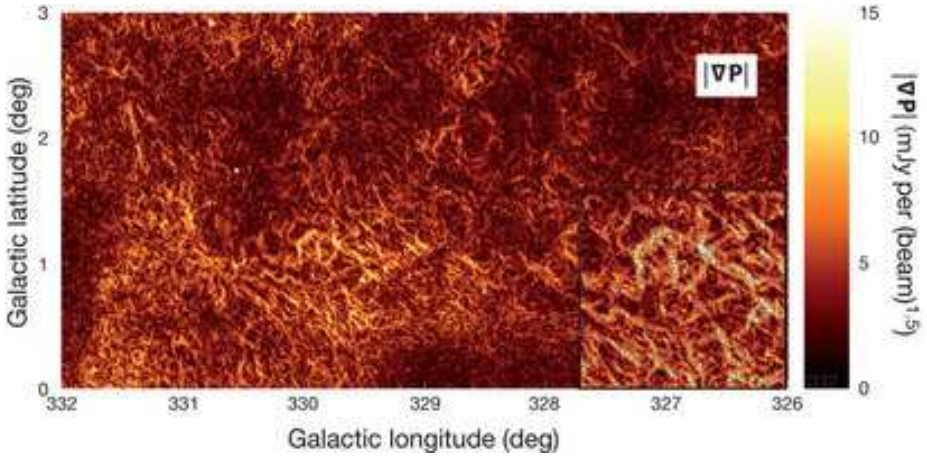

Fig. 6 The map of gradient of linear polarization $|\nabla \mathbf{P}|$ as defined in equation 17 for a field around the Galactic plane. The inset panel shows a $0.9° \times 0.9°$ close-up of the brightest structure in $|\nabla \mathbf{P}|$, where the direction of the gradient is plotted only for strong (> 5 mJy beam$^{1.5}$) gradient amplitudes. Figure reproduced from Gaensler et al. (2011).

These polarization gradient filaments can be characterized by the moments of the polarization gradient distribution. Simulations of magnetohydrodynamic (MHD) turbulence show that the third and fourth order moments (skewness γ and kurtosis β) increase monotonically with Mach number and depend on sonic Mach number. Comparison of the observed values $\gamma = 0.3$ and $\beta = 0.9$ with simulated values for varying sonic Mach numbers indicates that the magnetic turbulence in the ISM (at least in the field given in Figure 6) is mildly subsonic to transonic (Gaensler et al. 2011). This is in agreement with estimates of the sonic Mach number in the warm ionized medium from emission measure distributions (Hill et al 2008).

Simulations also show that the filaments in polarization gradients can be caused by either interacting shocks or random fluctuations in MHD turbulence (Burkhart et al 2012). These authors also introduce the genus method to characterize the polarization gradient maps. For subsonic turbulence as in the ISM, where magnetic field fluctuations dominate the polarization gradient topology, the topology is 'clumpy', as opposed to supersonic turbulence which shows a 'swiss cheese' topology.

6 Mysteries of Interstellar Turbulence

In the paper to this point, we have reviewed the remarkable amount of information revealed by radioastronomical studies on turbulence in the ISM. However, there remain a number of phenomena and effects that are not understood. In this section, we present what may be considered an agenda for future ISM radio propagation studies, that might clarify these issues. We discuss topics in which additional measurements may contribute in a major way to advances in our understanding of interstellar turbulence, or cases in which emerging observational results appear difficult to understand, given our current vision of the interstellar medium and the turbulence in it. These "mysteries" often involve input from the theory of plasma turbulence, and frequently rely on the latest results in this field. In other cases, they represent known observational results of long standing that have eluded explanation.

6.1 The Existence of a Cascade in Interstellar Turbulence

Is there really a cascade in interstellar turbulence from the outer scale of 4 parsecs (or 100 pc) to the dissipation scale of order $100 - 500$ km? Even in the case of well-studied solar wind turbulence this issue is not entirely resolved. Observations of solar wind turbulence indicate that it is comprised of Alfvèn waves propagating in both directions with respect to the large scale interplanetary magnetic field, i.e. towards and away from the Sun[3]. Within the context of the most commonly discussed theories of solar wind turbulence, these counterpropagating waves are necessary for the existence of nonlinearities that produce the turbulent cascade. In the case of the interstellar medium, we do not have observations sufficient to say if counterpropagating Alfvèn waves are present, and it is not clear how

[3] A more precise and technical statement would be that both the positive and negative "Elsasser Variables" are present in solar wind turbulence.

such a discrimination could be done. In fact, it is not even clear that interstellar turbulence can be described as an ensemble of Alfvèn waves.

6.2 Do We Understand the Flat RM Structure Functions?

Rotation Measure structure functions should have a logarithmic slope of 5/3 if both density and magnetic field fluctuations have a Kolmogorov spectrum, and an observationally indistinguishable value of 3/2 if a Kraichnan spectrum applies. This results holds if the two lines of sight are separated by a distance which is in the inertial subrange of the turbulence. Such a slope is rarely measured; a number of independent investigations have found that the RM structure functions on angular lags of several tenths of a degree to several degrees have logarithmic slopes of $\sim 1/2$, or even flatter.

The interpretation of this result has been that the angular lags probed correspond to large scales in the interstellar medium, of order the outer scale or larger (Minter & Spangler 1996; Haverkorn et al 2006, 2008). Minter & Spangler (1996) suggest that the aforementioned data are probing 2D turbulence that exists in sheets, and that the fully 3D component of the turbulence is on spatial scales less than the thickness of these sheets, with corresponding angular scales of order a few tenths of a degree or less. These analyses are, in fact, the basis of the claim that the outer scale is of order 1 - 5 parsecs in extent.

Nonetheless, it would be comforting to actually measure, in a clear and unambiguous fashion, the transition from a $\sim 1/2$ logarithmic slope on angular lags $\geq 1^\circ$ to $\sim 5/3$ on angular lags $\leq 0.2^\circ$. This would securely establish the value of the outer scale in the WIM turbulence. Without such measurements, we will continue to be tormented by the specter of on ISM in which we *are* measuring the inertial range of the turbulence (assuming this to be a meaningful concept), and that we lack an explanation for its logarithmic slope.

6.3 What is the Significance of the "Pulsar Arcs"

One of the most intriguing developments of the last decade in the study of interstellar turbulence has been the discovery of "pulsar arcs" (Walker et al 2004; Cordes et al 2006). The interpretation of this phenomenon seems to require that the turbulence responsible for interstellar turbulence is confined to one, or at most, a few thin sheets. A recent overview of the observational properties of the arcs and their interpretation is given in Rickett (2011). Is interstellar turbulence really confined to thin sheets? If so, what is the physical mechanism for the formation of them? If not, how are the Pulsar Arcs formed?

6.4 What Generates Interstellar Turbulence?

Plasma turbulence, as revealed by the density fluctuations responsible for radio scintillations, appears to be very widely distributed in the interstellar medium. The question then arises as to the mechanism responsible for its generation. A general consensus holds that the free energy source is expanding supernova

remnants, stellar superbubbles, and expanding HII regions (Norman and Ferrara 1996; MacLow and Klessen 2004; Hill et al 2012). The small scale fluctuations that we detect in radio scintillations might be generated by baroclinic effects[4] at the expanding interfaces between supernova remnants, stellar bubbles, and the ISM. However, there may be a problem with the distribution or diffusion of turbulence throughout the ISM. Supernova remnants and stellar bubbles occupy a very small fraction of the ISM, and turbulent damping limits the extent to which turbulence can propagate from the generation site to locations throughout the WIM (Spangler 2007; Spangler et al 2011).

6.5 Removal of Fast Magnetosonic Waves from Interstellar Turbulence

Fast Magnetosonic waves are one of the three MHD wave modes, so one would expect them to comprise part of interstellar turbulence. However, it has been argued that they can only constitute a negligibly small fraction of the energy in interstellar turbulence. The argument is based on the rapid damping of Fast Mode waves on thermal ions for conditions appropriate to the Warm Ionized Medium. If a sizeable fraction of the energy in interstellar turbulence is in the form of Fast Mode waves, then the large power input to the interstellar medium would exceed the cooling capacity of the WIM gas (Spangler 1991, 2003). Interestingly enough, they also seem to be absent from the solar corona and the solar wind at 1 a.u.. Harmon and Coles (2005) make a convincing argument that a substantial contribution of Fast Mode waves to the coronal turbulence budget is incompatible with spaced-receiver propagation measurements. Klein et al (2012) also argue that Fast Modes waves, or fluctuations possessing Fast Mode properties, constitute an insignificant portion of solar wind turbulence at 1 a.u.. The analysis of Klein et al (2012) is based on calculations of simulated turbulence, consisting of a superposition of Fast Mode waves, Slow Mode waves, and Alfvén waves. These simulated realizations of turbulence are compared with actual measurements of solar wind turbulence, especially the density-magnetic field correlation function. Klein et al (2012) find that the realizations that resemble the true, observed turbulence are those with an insignificant fraction of Fast Mode waves. It should be mentioned before leaving this topic that the absence of Fast Mode waves in heliospheric plasmas is a characteristic of plasmas far from shocks or other sources of unstable particle distributions. Shocks produce ion streaming instabilities which, in turn, generate beautiful, large amplitude Fast Magnetosonic waves, the best known examples of which are the waves upstream of the Earth's bow shock (see Hoppe et al 1981, for an entry point to a large literature). However, it seems to be the case that these Fast Mode waves are confined to relatively thin layers that bound strong shocks in the solar wind. To conclude this subsection, whether such a minor role for the Fast Mode in astrophysical turbulence is due to enhanced damping, or the turbulence generation mechanisms remains to be determined by future research.

[4] Baroclinic effects involve the generation of fluid vorticity by misaligned gradients of pressure and density.

6.6 Do We Understand the Lack of a Spectral Break at the Ion-Neutral Collisional Scale?

As discussed in Section 3.1, there is observational evidence for a power law spectrum of interstellar turbulence from scales of at least a few parsecs, down to scales as small as 100 km. The existence of a power law spectrum seems to indicate, on general grounds of dimensional analysis, that there are no fundamental scales between the outer scale on which stirring is done, and the inner scale where dissipation occurs. This assumption is in stark contrast to the situation for the WIM phase of the interstellar medium, in which a fundamentally-defined scale, the collisional scale $l_c \equiv \frac{V_A}{\nu_{in}}$, where V_A is the Alfvén speed and ν_{in} is the ion-neutral collisional scale, lies between the inner and outer scales ($l_c \simeq 10^{15} - 10^{16}$ cm). This conundrum was discussed by Armstrong et al (1995).

Cho and Lazarian (2003, this paper also contains references to earlier results by these authors) and Oishi and MacLow (2006) present numerical simulations showing that irregularities exist on scales smaller than the collisional scale, and conclude that ion-neutral collisional effects do not truncate the turbulent cascade. A different conclusion apears to be reached by Shaikh and Zank (2008). Shaikh and Zank (2008) find that while the turbulent cascade continues at wavenumbers larger than that corresponding to the ion-neutral collisional scale, the fundamental physics of the nonlinear interaction is modified. These authors claim that the magnetic field and velocity power spectra of the ionized fluid are significantly steepened in comparison with the same spectra of a fully-ionized plasma. This result would seem to be discordant with the observed Kolmogorov spectrum of density fluctuations down to much smaller spatial scales. This topic deserves further attention by the interested community.

6.7 The Outer Scale of Interstellar Turbulence and Cosmic Ray Propagation

In Section 3.6 above, we noted that several independent investigations find that the outer scale of turbulence in the WIM must be of order a few parsecs. There is an associated curiosity that was raised in Spangler (2001), but does not appear to have been discussed since. If there is a break in the turbulence corresponding to an outer scale of 4 parsecs, then there should be an associated change in the transport properties of cosmic rays which are resonant with such irregularities, i.e. those with energies of $10^{15} - 10^{16}$ eV. In fact, the famous "knee" in the cosmic ray spectrum occurs here, but other mechanisms are normally invoked for its existence. Should the change in turbulence properties at scales that resonate with such cosmic rays be added to the mechanisms considered? In considering this matter, it should be recognized that the outer scale of turbulence in the Galactic halo is probably large, of order 100 pc (see Section 3.6 above). The larger fluctuations in the Galactic halo could resonate with higher energy cosmic rays than the smaller fluctuations in the WIM of the spiral arms. The fluctuations in the halo may dominate the Galactic transport of cosmic rays.

6.8 Can Observations Provide a Connection to Theories of Kinetic Processes in Turbulence?

One of the most intriguing recent developments in the study of plasma turbulence has been elucidation of the role of kinetic processes in turbulence (i.e. those described by the Vlasov equation rather than MHD), and the observational support for these ideas in spacecraft measurements of solar wind turbulence (see Alexandrova et al 2009, and Section 3.5 above). Can we provide similar evidence of kinetic processes in the interstellar medium? Do the same kinetic processes which appear crucial in the solar wind, such as Landau damping of kinetic Alfvén waves, play an important role in the interstellar medium? In kinetic damping processes, energy will flow to either ions or electrons, depending on which is resonant with the fluctuations being damped. However, observations of the WIM plasma, the best diagnosed astrophysical plasma, show temperature equilibration between electrons and different ion species (Haffner et al 2009). A similar situation occurs in the clouds of the Very Local Interstellar Medium, where the same temperature characterizes neutral atoms as well as several ions with different masses (and therefore cyclotron frequencies) (Spangler et al 2011).

6.9 Why is the Spectrum of Plasma Turbulence the Same in HII Regions, the Warm Ionized Medium, and the Solar Wind?

The Armstrong et al (1995) result of a Kolmogorov density fluctuation spectrum over several decades pertains to the WIM component of the interstellar medium, having been established from observations of relatively nearby pulsars and extragalactic radio sources whose lines of sight are at high galactic latitudes. Radio wave propagation measurements made on heavily-scattered lines of sight that pass through HII regions (e.g. Spangler and Cordes 1988; Molnar et al 1995) are also consistent with a Kolmogorov density spectrum. Finally, the plasma of the solar corona and inner solar wind also has a Kolmogorov spectrum, particularly in the slow solar wind. The spectra of magnetic field and flow velocity also possess inertial subranges with spectra that are close to Kolmogorov, although recent research points to a slight difference in the power law indices of the magnetic field and velocity spectra (Boldyrev et al 2011). This result is, perhaps, somewhat unexpected since the mechanisms for generation of the turbulence at the outer scale are presumably quite different in these different media, as might be the plasma β that determines the dissipation mechanisms. Is the similarity of the turbulence in these quite different media a consequence of the universality turbulence?

7 Summary and Conclusions

Radio propagation observations yield a surprising amount of quantitative information about the plasma state of the interstellar medium, particularly turbulence in the WIM phase of the ISM and HII regions. The measurements emphasized in this paper have been Faraday rotation of linearly polarized signals that have propagated through the ISM during the passage from extragalactic radio sources

to the Earth, frequency-dependent polarization characteristics of the Galactic synchrotron radiation, and scintillations of Galactic and extragalactic radio sources due to small scale density fluctuations in the ISM. From this information, we can deduce the amplitude and spectral properties of interstellar turbulence. We have information on the outer and inner scales of this turbulence; the corresponding inertial subrange extends over roughly 10 decades. In some respects, interstellar turbulence resembles the extensively studied turbulence in the solar wind. However, there appear to be significant differences as well. In spite of impressive progress in this field, there are several (at least) poorly-understood aspects of interstellar turbulence that warrant the term "mysteries". Several of these aspects are discussed in Section 6 above. Some of these could be addressed in a significant way with new observations on new or substantially upgraded radio telescopes such as the VLBA and LOFAR.

Acknowledgements This work was supported at the University of Iowa by grants AST09-07911 and ATM09-56901 from the National Science Foundation of the United States. M.H. acknowledges the support of research programme 639.042.915, which is partly financed by the Netherlands Organisation for Scientific Research (NWO). The authors acknowledge the work of Jacob J. Buffo of the University of Iowa in the analysis of model structure functions, contained in Figures 4 and 5. We also thank James Cordes of Cornell University for providing the beautiful pulsar dynamic spectrum in Figure 1 as an illustration of one of the phenomena of radio wave propagation in a random medium.

References

Alexandrova, O. et al 2009, Phys. Rev. Lett. 103, 165003
Armstrong, J.W., Rickett, B.J., and Spangler, S. R. 1995, Astrophys. J. 443, 209
Beck, R. 2001, Space Sci. Rev., 99, 243
Beck, R., Frick, P., Stepanov, R., & Sokoloff, D. 2012, Astron. Astrophys., 543, A113
Bernardi, G., de Bruyn, A. G., Brentjens, M. A., Ciardi, B., Harker, G., Jelić, V., Koopmans, L. V. E., Labropoulos, P., Offringa, A., Pandey, V. N., Schaye, J., Thomas, R. M., Yatawatta, S., Zaroubi, S. 2009, A&A, 500, 965
Boldyrev, S., Perez, J.C., Borovsky, J.E., and Podesta, J.J. 2011, Astrophys. J. 741, L19
Brentjens, M. A., & de Bruyn, A. G. 2005, A&A, 441, 1217
Brentjens, M. A. 2011, A&A, 526, A9
Brisken, W.F. et al 2010, Astrophys. J. 708, 232
Brower, D.L. et al 2002, Phys. Rev. Lett. 88, 185005
Brown, J. C., Haverkorn, M., Gaensler, B. M., et al. 2007, Astrophys. J., 663, 258
Brown, M.R., Cothran, C.D., Landreman, M., Schlossberg, D., and Matthaeus, W.H. 1989, Astrophys. J. 577, L63
Bruno, R. and and Carbone, V. 2005, Living Reviews Solar Phys. 2,4
Burkhart, B., Stanimirovic, S., Lazarian, A., and Kowal, G. 2010, Astrophys. J. 708, 1204
Burkhart, B., Lazarian, A., & Gaensler, B. M. 2012, Astrophys. J., 749, 145
Burn, B. J. 1966, MNRAS, 133, 67
Carter, T.A., Brugman, B., Pribyl, P., and Lynbarger, W. 2006, Phys. Rev. Lett. 96, 155001
Cho, J. and Lazarian, A. 2003, Mon. Not. Royal Astr. Soc. 345, 325
Chen, C.H.K., Salem, C.S., Bonnell, J.W., Mozer, F.S., and Bale, S.D. 2012, Phys. Rev. Lett. 109, 035001
Chepurnov, A. and Lazarian, A. 2010, Astrophys. J. 710, 853
Chepurnov, A., Lazarian, A., Stanimirovic, S., Heiles, C., and Peek, J.E.G. 2010, Astrophys. J. 714, 1398
Coles, W.A. and Harmon, J.K. 1989, Astrophys. J. 337, 1023
Cordes, J.M., Weisberg, J.W., and Boriakoff, V. Astrophys. J. 288, 221-247 (1985)
Cordes, J.M. 1986 Astrophys. J. 311, 183

Cordes, J.M., Rickett, B.J., Stinebring, D.R., and Coles, W.A. Astrophys. J. 637, 346-365 (2006)
Crutcher, R.M., Wandelt, B., Heiles, C., Falgarone, E., and Troland, T. 2010, Astrophys. J. 725, 466
Ding, W.X. et al 2003, Phys. Rev. Lett. 90, 035002
Ferrière, K. 1998, Astrophys. J. 497, 759
Fey, A.L., Spangler, S. R. and Mutel, R.L. 1989, Astrophys. J. 337, 730
Fey, A.L., Spangler, S. R. and Cordes, J.M. 1991, Astrophys. J. 372, 132
Gaensler, B. M., Haverkorn, M., Burkhart, B., et al. 2011, Nature, 478, 214
Grall, R.R., Coles, W.A., Spangler, S.R., Sakurai,T., and Harmon, J.K. 1997, J.Geophys.Res. 102, 263
Haffner, L.M. et al 2003, Astrophys. J. Supp. 149, 405
Haffner, L.M. et al 2009, Rev. Mod. Phys. 81, 969
Harmon, J.K. 1989, J. Geophys. Res. 94, 15399
Harmon, J.K. and Coles, W.A. 2005, J. Geophys. Res. 110, A03101
Haverkorn, M., Katgert, P., & de Bruyn, A. G. 2000, A&A 356, L13
Haverkorn, M., Katgert, P., & de Bruyn, A. G. 2003, A&A, 404, 233
Haverkorn, M., Gaensler, B. M., McClure-Griffiths, N. M., Dickey, J. M., & Green, A. J. 2004, Astrophys. J. 609, 776
Haverkorn, M., Katgert, P., & de Bruyn, A. G. 2004, A&A, 427, 549
Haverkorn, M., Gaensler, B. M., Brown, J. C., Bizunok, N. S., McClure-Griffiths, N. M., Dickey, J. M., & Green, A. J. 2006, Astrophys. J. 637, L33
Haverkorn, M., Brown, J.C., Gaensler, B.M., and McClure-Griffiths, N.M. 2008, Astrophys. J. 680, 362
Haverkorn, M. 2013, in "Magnetic Fields in Diffuse Media", eds. Elisabete Gouveia dal Pino and Alexander Lazarian
Heiles, C. 2011, Bull. Am. Astr. Soc. 43, 21713208
Hill, A. S., Benjamin, R. A., Kowal, G., et al. 2008, Astrophys. J., 686, 363
Hill, A.S. et al 2012, Astrophys. J. 750, 104
Hoppe, M.M., Russell, C.T., Frank, L.A., Eastman, T.E., and Greenstadt, E.W. 1981, J.Geophys.Res. 86, 4471
Howes, G.G. et al 2008, J. Geophys. Res. 113, A05103
Howes, G.G., TenBarge, J.M., and Dorland, W. 2011 Phys. Plasm. 18, 102305
Howes, G.G. et al 2011, Phys. Rev. Lett. 107, 035004
Iacobelli, M., Haverkorn, M., & Katgert, P. 2013, Astron. Astrophys., 549, A56
Jokipii, J.R. 1977, Proceedings of the 15th International Cosmic Ray Conference 1, 15
Jokipii, J.R. 1988, in Radio Wave Scattering in the Interstellar Medium, American Institute of Physics Conference Proceedings 174, 48
Klein, K.G. et al 2012, Astrophys. J. 755, 159
Lazaryan, A. L., & Shutenkov, V. P. 1990, SvAL, 16, 297L
Lazio, T.J.W., Cordes, J.M., de Bruyn, A.G., and Marquart, J.P. 2004, New Astro. Rev. 48, 1439
Lee, L.C. and Jokipii, J.R. 1975, Astrophys. J. 196, 695
MacLow, M.-M. 2004, Astroph. and Space Science, 289, 323
MacLow, M.M. and Klessen, R.S. 2004, Rev. Mod. Phys. 76, 125
Malkov M. A., Diamond P. H., Drury L., & Sagdeev R. Z. 2010, ApJ 721, 705
Mao, S. A., Gaensler, B. M., Haverkorn, M., et al. 2010, Astrophys. J., 714, 1170
Molnar, L.M., Mutel, R.L., Reid, M.J., and Johnston, K.J. 1995, Astrophys. J. 438, 708
Minter, A. H. & Spangler, S. R. 1996, Astrophys. J. 458, 194
Norman, C.A. and Ferrara, A. 1996, Astrophys. J. 467, 280
Oishi, J.S. and MacLow, M.M. 2006, Astrophys. J. 638, 2810
Ohno, H., & Shibata, S. 1993, MNRAS, 262, 953
Patrikeev, I., Fletcher, A., Stepanov, R., et al. 2006, Astron. Astrophys., 458, 441
Pizzo, R. 2010, PhD thesis Groningen University.
Rae, K. M., & Brown, J. C. 2010, Astronomical Society of the Pacific Conference Series, 438, 229
Rickett, B.J. 1977, Ann Rev. Astr. Ap. 15, 479
Rickett, B.J. 1990, Ann Rev. Astr. Ap. 28, 561
Rickett, B.J., Johnston, S., Tomlinson, T., and Reynolds, J. 2009, Mon. Not. Roy. Astr. Soc. 395, 1391

Rickett, B.J. 2011, Am. Inst. Phys. Conf. Proc. 1366, 107
Sahraoui, F., Belmont, G., and Goldstein, M.L. 2012, Astrophys. J. 748, 100
Schnitzeler, D. H. F. M., Katgert, P. & de Bruyn, A. G. 2009, A&A, 494, 611
Shaikh, D. and Zank, G.P. 2008, Astrophys. J. 688, 683
Shukurov, A., & Berkhuijsen, E. M. 2003, MNRAS, 342, 496
Spangler, S. R. and Cordes, J.M. 1988, Astrophys. J. 332, 346
Spangler, S.R. 1988, Am. Inst. Phys. Conf. Proc. 174, 32
Spangler, S. R. and Gwinn, C.W. 1990, Astrophys. J. 353, L29
Spangler, S. R. 1991, Astrophys. J. 376, 540
Spangler, S. R. and Sakurai, T. 1995, Astrophys. J. 445, 999
Spangler, S. R. and Cordes, J.M. 1988, Astrophys. J. 505, 766
Spangler, S.R. 1999, Astrophys. J. 522, 879
Spangler, S.R. 2001, Space Sci. Rev. 99, 261
Spangler, S.R. et al 2002, Astron. Astrophys. 384, 654
Spangler, S.R. 2003, Astron. Astrophys. 407, 563
Spangler, S.R. 2007, Astro. Soc. Pac. Conf. Proc. 265, 307
Spangler, S.R. 2009, Space Sci. Rev. 143, 277
Spangler, S.R., Savage, A.H., and Redfield, S. 2011, Am. Inst. Phys. Conf. Proc. 1366, 97
Spangler, S.R., Savage, A.H., and Redfield, S. 2011, Astrophys. J. 742, 30
Strauss, H.R. 1976, Phys. Fl. 19, 134
Tatarski, V.I. 1961, Wave Propagation in a Turbulent Medium (McGraw Hill: New York)
Thomson, R. C., & Nelson, A. H. 1980, MNRAS, 191, 863
Thompson, A.R., Moran, J.M., and Swenson, G.W., Jr. 1986, *Interferometry and Synthesis in Radio Astronomy*, Wiley & Sons, New York
Tielens, A. G. G. M. 2005, *The Physics and Chemistry of the Interstellar Medium*, Cambridge University Press, p14
Uscinski, B.J. 1977, *The Elements of Wave Propagation in Random Media*, McGraw-Hill
Van Eck, C. L., Brown, J. C., Stil, J. M., et al. 2011, Astrophys. J., 728, 97
M.A. Walker, D.B. Melrose, D.R. Stinebring, and C.M. Zhang, MNRAS 354, 43-53 (2004)
Yamada, M., Kulsrud, R., and Ji, H. 2010, Rev. Mod. Phys. 82, 603
Whiting, C.A., Spangler, S.R., Ingleby, L.D., and Haffner, L.M. 2009, Astrophys. J. 694, 1452
Wolleben, M., Landecker, T. L., Carretti, E., Dickey, J. M., Fletcher, A., Gaensler, B. M., Han, J. L., Haverkorn, M., Leahy, J. P., McClure-Griffiths, N. M., McConnell, D., Reich, W., Taylor, A. R. 2009, IAU Symposium, 259, 89
Zweibel, E.G. and Yamada, M. 2009, Ann. Rev. Astr. Ap. 47, 291